Article

Treatment of Flue Gas in a CO₂ Capture Pilot Plant for a Commercial CFB Boiler

Izabela Majchrzak-Kucęba [1,*] **, Dariusz Wawrzyńczak** [1] **, Janusz Zdeb** [2] **, Wojciech Smółka** [2] **and Artur Zajchowski** [2]

[1] Department of Advanced Energy Technologies, Faculty of Infrastructure and Environment, Czestochowa University of Technology, Dabrowskiego Street 73, 42-201 Czestochowa, Poland; dariusz.wawrzynczak@pcz.pl

[2] TAURON Wytwarzanie S.A., Promienna Street 51, 43-603 Jaworzno, Poland; Janusz.Zdeb@tauron-wytwarzanie.pl (J.Z.); Wojciech.Smolka@tauron-wytwarzanie.pl (W.S.); Artur.Zajchowski@tauron-wytwarzanie.pl (A.Z.)

* Correspondence: izabela.majchrzak-kuceba@pcz.pl; Tel.: +48-343250463

Abstract: The problem of reducing carbon dioxide emissions from flue gas, particularly from flue gas originating from coal-firing CFB systems, is currently an important challenge. Many centers around the world have tested post-combustion CO₂ capture systems. One of these systems, operated using DR-VPSA adsorption technology (dual-reflux vacuum pressure swing adsorption), was tested under the Strategic Project in Poland. The flue gas in this study originated from a supercritical CFB boiler (460 MWe). An important problem involved in capturing CO₂ from flue gas is the occurrence of SO₂ and NOₓ. These substances have a negative effect on the CO₂ adsorption process. In this study, commercial impregnated activated carbon was used to remove SO₂ and NOx from CFB flue gas in the pre-treatment section during the tests of a pilot CO₂ capture unit in a large-scale CFB boiler at the Lagisza Power Plant (Poland). The spent activated carbon was analyzed using several different methods (N₂ adsorption–desorption isotherms, SEM-EDX, XRD, FTIR, and TG) to evaluate the efficiency of the operation and life span of the adsorbent used in the SO₂ and NOₓ removal unit. The results demonstrate that using commercial impregnated activated carbon in the pre-treatment section ensures sufficient flue gas purification and the removal of sulfur oxides but remains insufficient for nitrogen oxides.

Keywords: flue gas; CO₂ capture; DR-VPSA; CFB boiler; SO₂/NOₓ removal

1. Introduction

Reducing the emissions of CO₂ and other greenhouse gases contributing to global warming is a global challenge. Among the many proposed CO₂ emission reduction solutions is CCSU (carbon capture and storage/utilization), which enables CO₂ to be captured and then stored or utilized by processing it into a usable product such as methanol using renewable energy sources [1,2]. The most developed and advanced CO₂ capture technologies are amine-based absorption systems such as the large-scale absorption units operating at the coal-fired Boundary Dam power plant in Canada and at the coal-fired Petra Nova power plant in Texas in the United States [2]. Another dynamically developing CO₂ capture technology is the solid adsorbent-based adsorption technique involving vacuum pressure swing adsorption (VPSA) technology [3–9]. To date, at a pilot scale and under real power plant conditions, adsorption units for CO₂ capture on fixed beds have been tested in Japan [4,5], China [6], Australia [7], and Poland [8,9]. According to the tests carried out on all pilot adsorption CO₂ capture units treating real flue gas [4–9], one of the most important factors influencing the effectiveness of CO₂ adsorption is the content of H₂O and other impurities such as SO₂, NOₓ, dust, alkalis, and volatile metals in the flue gas [10–16]. These components have negative effects on the physical adsorbents

used in the adsorption method (activated carbon [4–9,17–19], zeolites [4–9], metal–organic frameworks [20,21], and mesoporous silica [22]), thereby reducing their CO_2 sorption capacity, which affects CO_2 purity and recovery. Meanwhile, many growing present-day recycling methods for CO_2 captured from power plants and other branches of industry require clean CO_2 streams. Moreover, the presence of the above-listed impurities accelerates deactivation of the CO_2 adsorbent, making more frequent replacement of the adsorbent necessary and thus increasing total costs of capturing CO_2 from flue gas. Therefore, it is important to ensure the effective removal of SO_2 and NO_x from flue gas before the CO_2 adsorption process because both SO_2 and NO_x can adsorb and/or react with CO_2 adsorption materials [10–19]. Similar to amine-based absorption systems [23], the SO_2 and NO_x content in flue gas should be ca. 10 mg/Nm^3 before the flue gas is sent to the CO_2 adsorption unit, while the limits of SO_2 and NO_x emissions from flue gas needed for coal power plants in the EU are now 200 mg/Nm^3 [24]. As a result, all pilot CO_2 separation units described in the literature comprise pre-treatment sections designed to dry and purify flue gas, which primarily involves the removal of SO_2 and NO_x before it is sent to the CO_2 capture section. This assignment is impacted by using various methods and adsorbents (Figure 1). Regrettably, there is little information concerning the functioning of these units, their efficiency, and the effectiveness of adsorbents used to remove SO_2 and NO_x [4,7]. For flue gas drying alongside the removal of SO_2 and NO_x in a pilot VPSA CO_2 capture unit, Wang et al. [6] proposed a pre-treatment unit consisting of a two-column TSA (temperature swing adsorption) module in which 156 kg of alumina was used as the adsorbent [6]. This adsorbent was also used by Ishibasi et al. as a packing material in a PSA (pressure swing adsorption) unit employed as the pre-treatment section for flue gas drying and additional SO_2 removal in an adsorption CO_2 capture unit [4,5]. Studies demonstrated that in addition to adsorbing moisture, the applied alumina also co-adsorbed CO_2. As a result of these tests, it was observed that in the primary stage, alumina acted as a moisture absorbent and also captured SO_2 in the form of sulfuric acid and aluminum sulfate, which was found in an adsorbent taken from the bottom part of the adsorption column. It was demonstrated that this result did not affect dryer efficiency. The SO_2 removal was so effective that no SO_2 accumulation was observed in the CO_2 adsorbent removed after 2000 h of use in a PTSA/PSA adsorption unit installed to capture CO_2. These studies confirmed that the applied alumina worked as both a moisture adsorbent and as a filter protecting against SO_2.
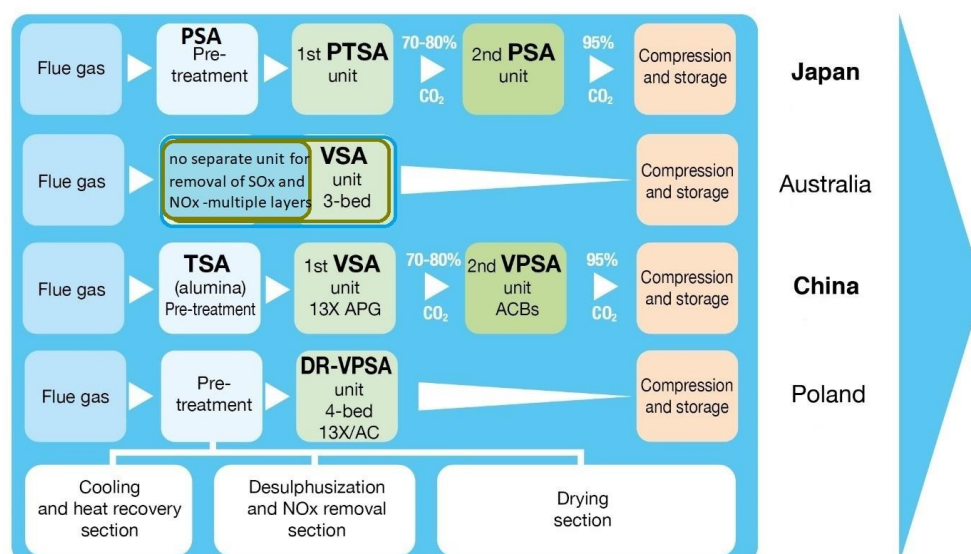
Figure 1. Pre-treatment sections in global pilot adsorption CO_2 capture units (PTSA: pressure temperature swing adsorption; PSA: pressure swing adsorption; VSA: vacuum swing adsorption; VPSA: vacuum pressure swing adsorption; DR-VPSA: dual-reflux vacuum pressure swing adsorption).

On the other hand, in the solution proposed by Qader et al. [7], no separate unit for the drying and removal of SO_2 and NO_x from flue gas was used, but the pre-treatment unit's function was affected by an adsorber column with multiple layers, removing $H_2O/SO_2/NO_x$ in the first layer of the adsorbent and CO_2 in the second layer [7]. Multi-layer adsorbents were applied in this solution: The first layer consisted of adsorbents used to remove water and SO_2/NO_x from flue gas, and the second consisted of adsorbents selective to CO_2. This system's functionality demonstrated that SO_2 and NO_x not captured from flue gas may cause blower corrosion induced by generated sulfuric acid. Thus, the elimination of SO_2, NO_x, and water from flue gas is required in the commercial use of adsorption installations for capturing CO_2 because these impurities may negatively affect the functionality of the installation elements. A different solution was employed in a Polish installation [8] where the pre-treatment section consisted of three different subsections: a cooling and heat recovery section, desulfurization and NO_x removal adsorbers, and a drying section. To date, only in this solution were far flue gas drying and the removal of SO_2 and NO_x carried out in separate sections. Another innovation was to use activated carbon impregnated with potassium hydroxide and potassium iodide for the simultaneous removal of SO_2 and NO_x [8]. This adsorbent was chosen because impregnated activated carbon was proposed, primarily for the simultaneous removal of SO_2 and NO_x. While the adsorption of gases on activated carbon is predominantly driven by physisorption, that of the modified carbon surface is driven by both physisorption and chemisorption. Modification of the AC surface is necessary to improve attraction between the adsorbent and target gases, resulting in a higher adsorption capacity of gases, especially at low gas concentrations in the flue gas. As an impregnating substance, KOH is known to have an excellent selective adsorption capacity for acid gases. An AC upgraded by impregnating it with KOH and KI promoted chemisorption with SO_2 and NO_x [25–30].

Moreover, no data are available on the use of activated carbon impregnated with KOH/KJ for the simultaneous removal of SO_2 and NO_x in pilot adsorption CO_2 capture installations under the operational conditions of large-scale CFB facilities. Valuable pilot plant data from commercial CFB units are presented in this work. Only a few studies have been devoted to the impacts of impurities such as SO_2 and NO_x on CO_2 adsorption by VSA (vacuum swing adsorption) [13] in the extant literature. Considering this factor, the present article focuses on assessing the efficiency of applied adsorbents in the removal of SO_2 and NO_x from flue gas prior to the CO_2 removal process at the Lagisza Power Plant. To assess the efficiency of using impregnated activated carbon in pre-treatment units to remove SO_2 and NO_x from CFB (circulating fluidized bed) flue gas, a comprehensive analysis of the adsorbents was carried out before and after their use in the desulfurization and NO_x removal section in a pilot adsorption (DR-VPSA) CO_2 capture unit under typical flue gas conditions. Studies of this type have not been reported in the CFB literature. Many articles discuss and focus on H_2O impacts on CO_2 sorption in adsorption installations, but there are no detailed analyses regarding effective SO_x and NO_x removal from flue gas. The available literature rarely reports real CFB flue gas treatments. Studies of this type would not only help us understand the principles of impurity adsorption and the efficiency of applied adsorbents but would also provide valuable data for the design of adsorption-based demonstration CO_2 capture installations. The purpose of the current research was to understand simultaneous SO_2 and NO_x adsorption on impregnated activated carbon at the stage of CFB flue gas pre-treatment in post-combustion CO_2 capture. Evaluation of the desulfurization/denitrification mechanism was performed through spent activated carbon post-analysis.

2. Experimental Section

2.1. Pre-Treatment Section in a Pilot-Scale DR-VPSA Carbon Capture Unit

In 2015–2016, under the Strategic Project financed by NCBiR (the National Centre for Research and Development) in Poland, research was carried out on post-combustion CO_2 capture in a pilot DR-VPSA mobile unit located at Tauron Wytwarzanie S.A.—The Lagisza

Power Plant in Poland. The flue gas originated from the world's first supercritical CFB boiler (460 MW$_e$). The mobile CO_2 capture unit consisted of a flue gas pre-treatment section and a carbon dioxide separation section (four-bed DR-VPSA) (Figure 2). In the proposed solution, a complex pre-treatment section was used for the first time and compared to other pilot CO_2 adsorption units [4–7]. The pre-treatment unit consisted of heat exchangers, an isothermal absorber, a deSO$_x$ and deNO$_x$ adsorber, and a glycolic gas dehydration system. The CO_2 separation unit consisted of four two-section adsorbers [8]. Detailed information about the mobile pilot DR-VPSA unit and the performed tests is available in previous studies [8,9]. The present article focuses only on the functionality of desulfurization and the NO$_x$ removal adsorber, which is an element of the flue gas pre-treatment section. More specifically, this study focuses on evaluating the desulfurization/denitrification mechanism through spent activated carbon post-analysis.
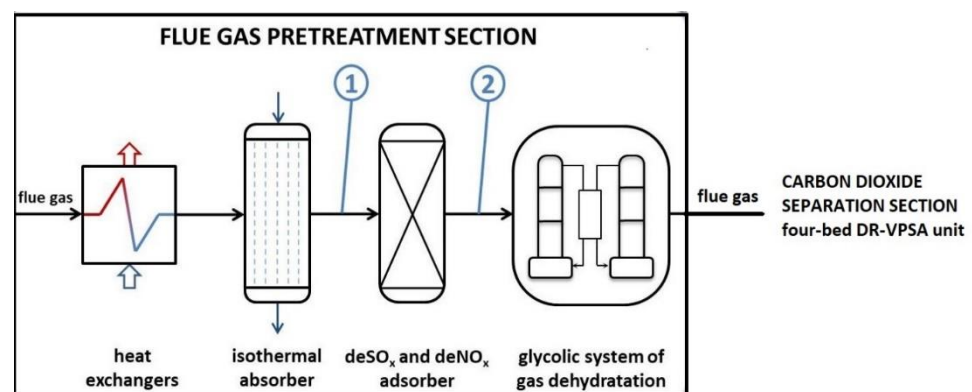

Figure 2. The scheme of the pilot DR-VPSA unit including the locations of the AC sample retrieval for analysis purposes (1, 2: flue gas drawing locations).

Before the flue gas generated in Lagisza Power Plant was sent to the pilot four-bed DR-VPSA unit, the following impurities were removed from the gas at the plant: SO_2, using a dry desulfurization method, and NO$_x$, using selective, non-catalytic reduction. The resulting average SO_2 and NO$_x$ content in the flue gas from the CFB boiler was as follows: SO_2 of 154.6 mg/Nm^3 and NO$_x$ of 179.8 mg/Nm^3 [8]. These content levels satisfy the applicable emission standards for these gases but remain too high for CO_2 capture units. As a result, the CO_2 capture installations need a pre-treatment section to reduce the SO_2 and NO$_x$ from the flue gas to ca. 10 mg/Nm^3. Effective SO_2 and NO$_x$ removal in this section is essential because this removal affects the purity of the CO_2 captured in the CO_2 separation unit [9], which is important for recycling the obtained CO_2 stream. Many of the proposed recycling methods require a high-purity CO_2 stream. For example, NO$_x$ can be a problem in the CO_2 stream if the stream is intended to be used in the food and beverage industry.

2.2. Characterization of the Adsorbent Used in the deSO$_x$ and deNO$_x$ Adsorber

Activated carbon (AC-P) Airpel 10 impregnated with potassium iodide KI (ca. 2 wt.%) and KOH (ca. 3 wt.%) manufactured by DESOTEC Activated Carbon was used for the simultaneous removal of SO_2 and NO$_x$ in the flue gas pre-treatment section pilot DR-VPSA CO_2 capture unit. This carbon (130 kg) was used as packing in the deSOx and deNOx adsorber (Figure 3). The activated carbon (AC-P) in this study was granulated activated carbon produced from anthracite with a pellet radius of >2.36 (99% mass), density of 520 kg/m^3, water vapor capacity of 40.1%, and a highly developed surface of 959 m^2/g. While the adsorption of gases on porous activated carbon is driven primarily by physical adsorption, in the case of a modified carbon surface (KOH), the adsorption of gases is driven by both physical adsorption and chemisorption with a chemical reaction between the surface function groups and adsorbed gases. AC surface modification is necessary to

improve the pull between the adsorbent and gases, especially when the gas concentration in flue gases is low. This type of modification is required to increase the alkalinity and general chemistry of the carbon surface under the pull of strongly polarized SO_2 gas. Potassium iodide performs the role of an "oxygen carrier". The $deSO_x$ and $deNO_x$ adsorber was designed to reduce SO_2 to ca. 10 mg/Nm^3 and NO_x to 40 mg/Nm^3. The $deSO_x$ and $deNO_x$ adsorber functioned continuously for 808 h in the pilot CO_2 capture installation (DR-VPSA) under the operational conditions of a large-scale CFB facility. The activated carbon (AC-P) samples were taken for analysis afterwards. Replacement of the AC-P sorbent that filled the $deSO_x$/$deNO_x$ adsorber was not necessary after 808 h of DR-VPSA operation because no increase was observed in the SO_2 concentration at the outlet of the column. If necessary, regeneration of the spent adsorbent was carried out using the activated carbon producer (DESOTEC Activated Carbon). Figure 3 shows the locations where activated carbon samples were retrieved for the tests (bottom, middle, and top of the adsorption column).
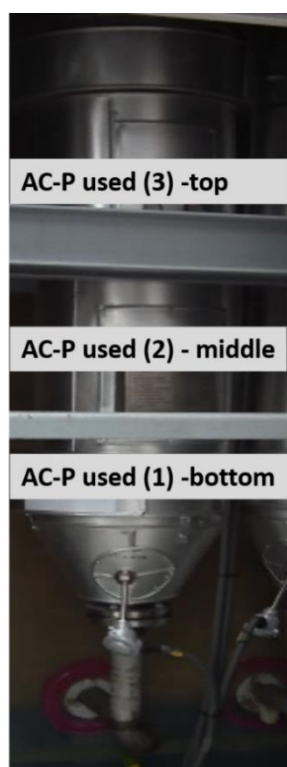
Figure 3. Retrieval locations for the activated carbon AC-P used as packing for the deSOx and deNOx adsorber in the pilot DR-VPSA CO_2 capture unit.

The spent activated carbon was analyzed using different methods (N_2 adsorption–desorption isotherms, SEM-EDX, XRD, FTIR, and TG) to evaluate the desulfurization/denitrification mechanism, efficiency of operation, and durability of the adsorbent used in the $deSO_x$ and $deNO_x$ adsorber. The impregnated activated carbon AC-P was also characterized before being used in the $deSO_x$ and $deNO_x$ adsorber. A Leco Elemental Analyser CHNS was used to assess the AC-P chemical composition. The porous properties of AC-P activated carbon after 808 h of use in deSOx and $deNO_x$ adsorber were assessed based on the N_2 adsorption–desorption isotherm at $-196\,°C$ using a Micromeritics model ASAP 2010. Prior to the measurements, the sample was outgassed at 473 K under an N_2 flow for at least 3 h. The BET method was then used to determine the specific surface area of the AC-P, and the BJH method was used to assess the pore-size distribution. Before and after adsorption, a surface chemical analysis of the sample was performed using SEM (EVO-40 Series, Carl Zeiss SMT electron microscope equipped with an energy dispersive X-ray spectroscope),

FTIR (Nicolet 6700 spectrometer), and XRD (X-ray diffractometer Panalytical X'PERT PRO). TG was performed using a Mettler TGA/DSC1 thermal analyzer. About 10 mg of the activated carbon was heated at 20 °C min^{-1} to 1000 °C with a flow ratio of nitrogen equal to 50 cm^3 min^{-1}. The online analysis of SO_2 and NO_x concentrations in the flue gas was carried out during the measuring tests of the pilot DR-VPSA unit installation with real CFB flue gas at the Lagisza Power Plant to complete the information obtained from analyzing the physicochemical properties of the impregnated activated carbon (AC-P) before and after its use in the $deSO_x$ and $deNO_x$ adsorber. The concentration of SO_2 and NO_x gases was registered before (point 1) and after the $deSO_x$ and $deNO_x$ adsorber (point 2) to continuously monitor the effectiveness of the process involving SO_2 and NO_x removal from the flue gas (Figure 2). During testing, gas samples were taken continuously using a multiplexer and directed to an analyzer equipped with an FTIR sensor to measure the SO_2 and NO_x concentrations. This analysis was also carried out in the CO_2 separation section to assess the effect of these impurities on the working efficiency of the CO_2 adsorbent and on the captured CO_2 purity. Detailed information on the results obtained in the CO_2 separation section is available in [9]. The present article focuses only on analyzing the SO_2 and NO_x content in flue gas at the inlet to the $deSO_x$ and $deNO_x$ adsorber and at the exit from the $deSO_x$ and $deNO_x$ adsorber.

3. Results and Discussion

3.1. Chemical Composition of the Spent Activated Carbon

The elemental chemical compositions of the fresh and used impregnated activated carbon AC-P in desulfurization and the NO_x removal adsorber are shown in Table 1. The primary differences in constitution between the fresh AC-P and the three used AC-Ps (retrieved from the bottom, middle, and top of the desulfurization unit) were their sulfur contents. Samples of used AC-P taken from the desulfurization unit had a notably higher S content (from 0.98 to 4.14 wt.%) compared to the fresh AC-P (0.29 wt.% S), which led to effective SO_2 adsorption from the flue gas under treatment, primarily in the lower part of the $deSO_x$ and $deNO_x$ adsorber (used AC-P (1)). Analysis of chemical composition also demonstrated that AC-P impregnated with KOH/KJ, which was used in the $deSO_x$ and $deNO_x$ adsorber, did not adsorb nitric oxides from treated gas and was not effective in this regard. In the samples of used AC-P retrieved from the $deSO_x$ and $deNO_x$ adsorber, no N content was observed to be higher than that in fresh AC-P.

Table 1. The elemental composition of the fresh and used activated carbon AC-P.

| Adsorbent	Elemental Composition				
	C, wt.%	H, wt.%	N, wt.%	S, wt.%	Other, O wt.%
fresh AC-P	72.34	1.80	0.86	0.29	24.71
used AC-P (1)—bottom	63.16	2.66	0.67	4.14	29.37
used AC-P (2)—middle	66.81	2.56	0.53	2.75	27.35
used AC-P (3)—top	69.86	2.44	0.73	0.98	25.99

3.2. Porous Structure of the Spent Activated Carbon

By analyzing data on the porous structure (Table 2) of the activated carbon before and after 808 h of use in the $deSO_x$ and $deNO_x$ adsorber, it was possible to observe changes in the specific surface area and volume and surface area of the pores. The specific surface area of AC-P after 808 h of use in the adsorber decreased for the used AC-P by 23.21%–42.11% (depending on the location of AC-P retrieval in the $deSO_x$ and $deNO_x$ adsorber) compared to fresh AC-P (whose specific surface was 959 m^2 g^{-1}). The volume of pores also decreased by 19.52% to 43.91% depending on the location of AC-P retrieval in the $deSO_x$ and $deNO_x$ adsorber). Moreover, the total area of pores in all spent AC-Ps decreased by 22.54–37.92% (Table 2). The spent samples had smaller specific surface areas and volumes of micropores, likely due to the presence of SO_2 adsorbed from the polluted flue gas and perhaps from

other impurities such as dust. The SO_2 adsorption process resulted in a decrease in the BET surface areas and pore volume of the activated carbon materials, indicating a blocking of pores due to clusters of new stable ionic crystals of K_2SO_3 and K_2SO_4. The degree of reduction in terms of both the area and the pore volume was the greatest for the used AC-P (1) taken from the lower part of the desulfurization unit. This used AC-P adsorbed the largest amount of SO_2 from the flue gas.

Table 2. Porous properties of the fresh and used impregnated activated carbon AC-P.

Sample	Textural Properties		
	BET Surface Area, $m^2\ g^{-1}$	Total Pore Volume, $cm^3\ g^{-1}$	Total Pore Area, $m^2\ g^{-1}$
fresh AC-P	959.00	0.41	739.30
used AC-P (1)—bottom	555.20	0.23	459.03
used AC-P (2)—middle	692.13	0.31	572.67
used AC-P (3)—top	736.46	0.33	515.95

Sulfur presence was also confirmed by analyzing the chemical composition of the samples (Table 1). Figure 4 presents the nitrogen adsorption–desorption isotherms (Figure 4a) and pore-size distributions (Figure 4b) for the activated carbon AC-P samples before and after use in the $deSO_x$ and $deNO_x$ adsorber. The adsorption/desorption isotherm of fresh AC-P was a type I isotherm, which confirmed the adsorbent's microporosity with a large number of mesopores, as demonstrated by the hysteresis loop starting at relative pressure (p/p_0) over 0.35. The adsorption/desorption isotherms of the used AC-P presented the same shapes, and differences in relation to fresh AC-P mainly applied to the volume of adsorbed nitrogen (Figure 4a).
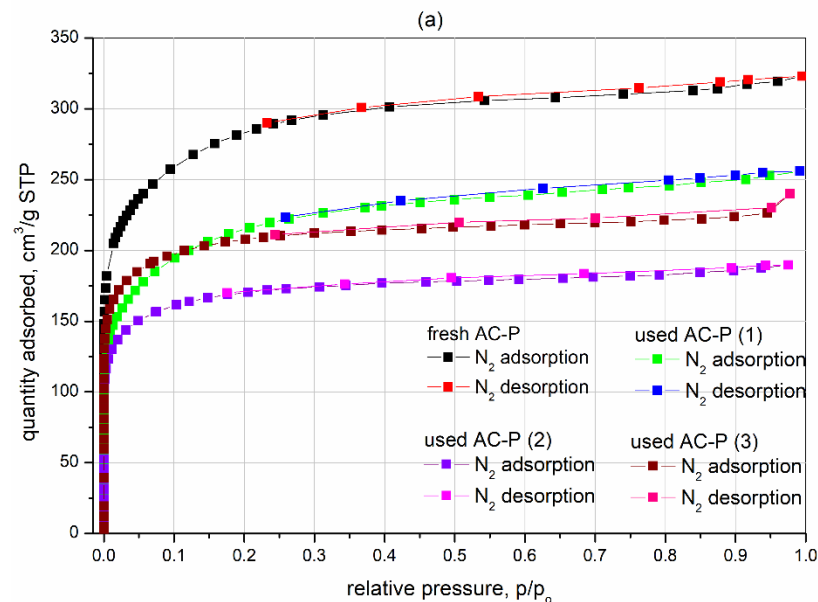
Figure 4. *Cont.*
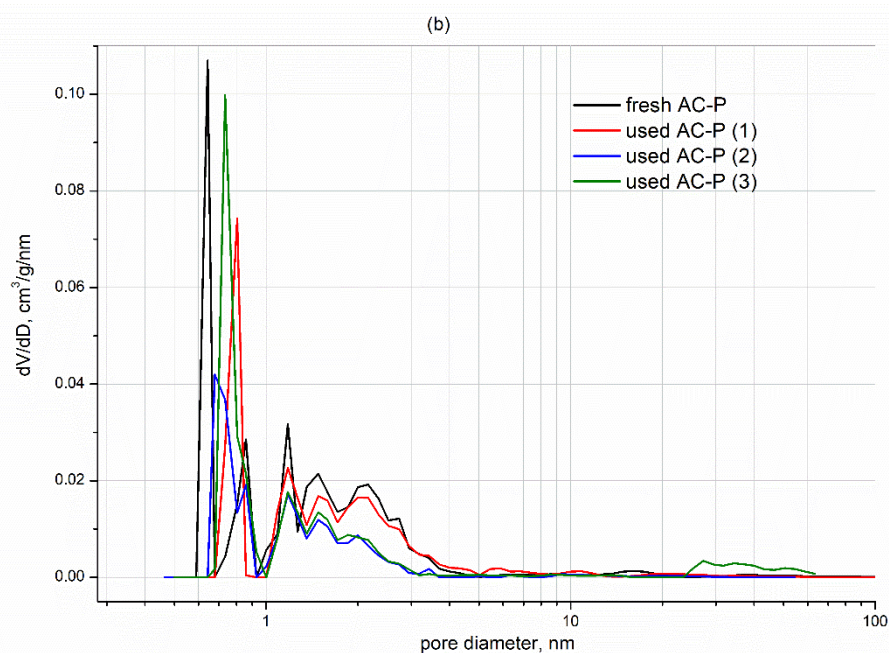
Figure 4. Nitrogen adsorption–desorption isotherms (**a**) and pore-size distributions (**b**) for activated carbon samples: fresh AC-P, used AC-P (1), used AC-P (2), and used AC-P (3).

This was demonstrated by the behavior of the porous structures of the used AC-P samples after 808 h of use in the desulfurization unit. As shown in Figure 4b, minor changes can also be observed in the pore-size distributions for the activated carbon AC-P samples, both fresh and used. This confirms the presence of minor changes in the porous structures of the AC samples after 808 h of using them to remove sulfur and nitrogen from flue gas before delivering the gas to the adsorption installation for CO_2 separation.

3.3. Microstructure of the Spent Activated Carbon

The presence of sulfur in the spent activated carbon AC-P was confirmed by SEM-EDX analysis, according to which the sulfur content was a maximum of 14.0 wt.% for used AC-P (3) retrieved from the adsorber top, 14.92 wt.% for used AC-P (2) retrieved from the adsorber middle, and 20.29 wt. % for used AC-P (1) from the adsorber bottom.

Figure 5 shows SEM photographs and the results of the SEM-EDX chemical constitution analysis on the surface of the impregnated activated carbon (both fresh and used) in the $deSO_x$ and $deNO_x$ adsorber. The observation of the microstructure in the tested AC-P samples confirmed the occurrence of new structures as a result of the use of the samples in the adsorber. Photographs of the spent AC-P showed crystals of sulfate and potassium sulfite formed as a result of SO_2 sorption. Most of the K_2SO_4 crystals were formed in the bottom of the desulfurization unit (used AC-P (1)), as demonstrated by the SEM photographs (Figure 5b) showing the greatest amount of potassium sulfate crystals. This result was also confirmed by analyzing the chemical composition on the surfaces of the activated carbons, which showed higher sulfur and potassium (K_2SO_3 and K_2SO_4) content compared to fresh AC-P in the AC-P samples retrieved after 808 h of use in the adsorber.

3.4. Surface Chemistry of the Spent Activated Carbon

Characterization of the FTIR spectra for sample surface chemistry was carried out to obtain information on changes in the functional groups on the AC-P surface before and after desulfurization and denitrification. Analysis of the FTIR spectra for fresh AC-P and AC-P after use in the adsorber, as presented in Figure 6, confirmed surface changes in the used AC-P due to SO_2 adsorption.
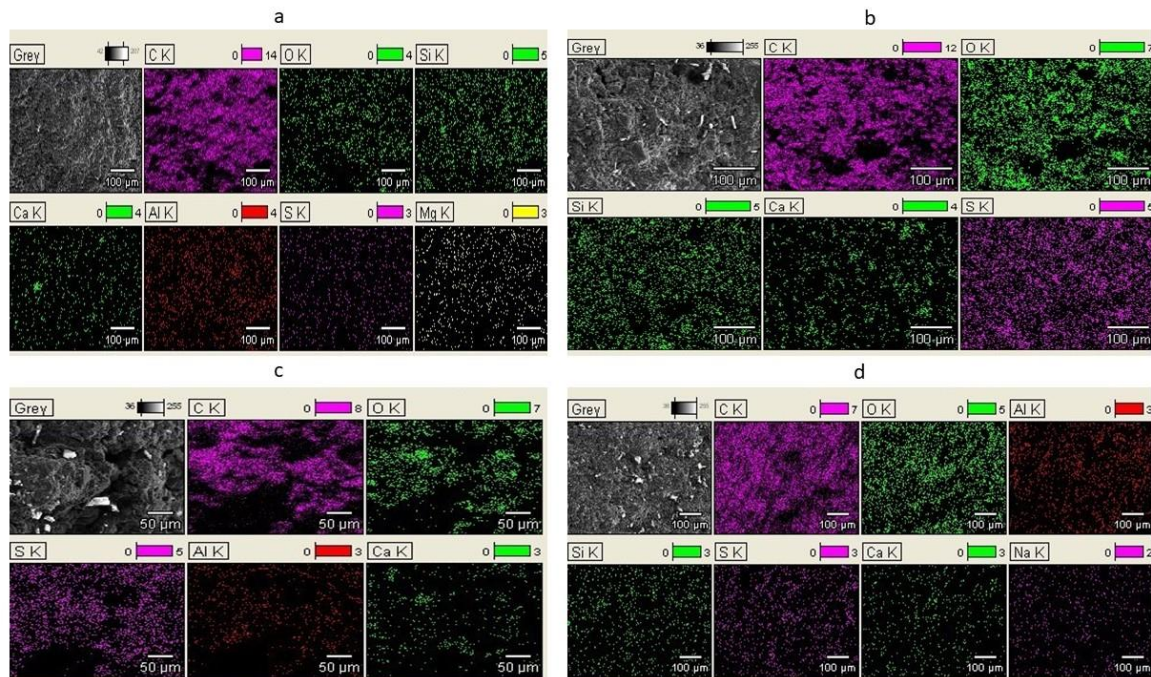
Figure 5. SEM-EDX analysis of activated carbon (fresh and used) in the deSO$_x$ and deNO$_x$ adsorber: (**a**) AC-P; (**b**) used AC-P (1); (**c**) used AC-P (2) and (**d**) used AC-P (3).
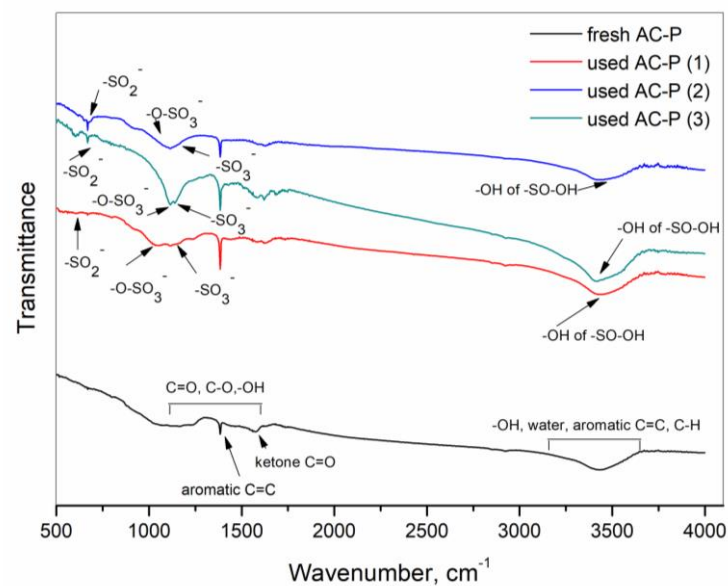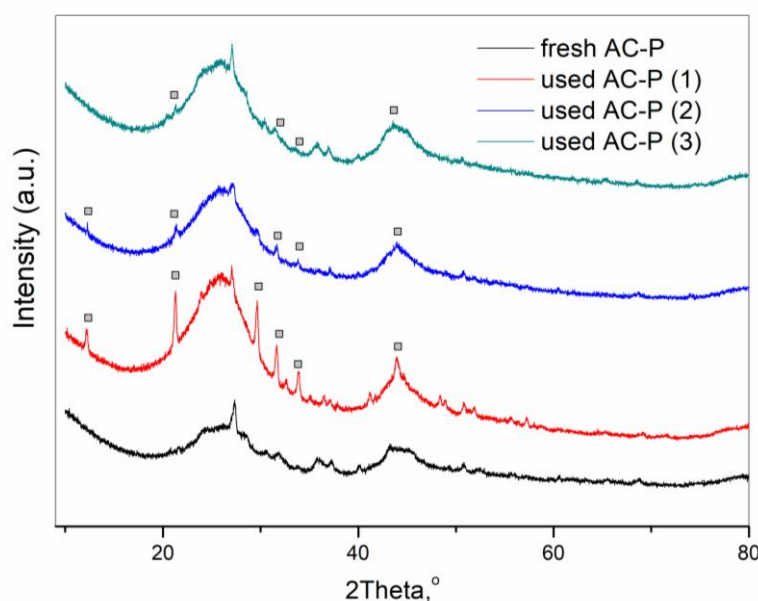

Figure 6. FTIR profiles of impregnated activated carbon: fresh and after use in the deSO$_x$ and deNOx adsorber: fresh AC-P, used AC-P (1), used AC-P (2), and used AC-P (3).

No observed changes indicated NO$_x$ adsorption. The fresh and used AC-P spectra showed characteristic peaks related to -OH vibrations at 1650 cm^{-1} and 3500 cm^{-1} due to the presence of the basic group -OH (originating from KOH and moisture). Moreover, at the 1800–1690 cm^{-1} wavelength, we observed a peak generated by the ketone group C=O and at 1630 cm^{-1} from the aromatic group C=C. Below 1600 cm^{-1}, we observed low-intensity peaks from the C=O, C-O, and -OH groups. Extra peaks appeared in the spectra of all used AC-P samples retrieved from the deSO$_x$ and deNO$_x$ adsorber, which confirmed changes on the surfaces of the spent activated carbons. The signals at 1150 cm^{-1} could be linked to sulfates generated after SO$_2$ adsorption (the strong band/spectrum of the

-OH group belonging to the -SO-OH group was generated during SO_2 adsorption on the AC-P at 3435 cm^{-1}, the band at 1159 cm^{-1} originated from the $-SO_3-$ group, and the strong band at 1113 cm^{-1} originated from the -O-SO_3- group) [28]. During the analysis of SO_2 adsorption on activated carbon with potassium hydroxide activation, many of the same groups were observed by Lee et al. [28]. No groups indicating the formation of nitrates were found on the surface of the used AC-P. Moreover, a weak band of the -SO_2- group appeared at 984 cm^{-1}. However, as emphasized by other authors [28], low-intensity peaks that induce microscopic changes via functional groups generated through SO_2 adsorption might become hidden or overlap and thus would not be observed. To sum up, during SO_2 adsorption, activated carbon impregnated with KOH works as a selective site of adsorption, with the OH- groups guaranteeing basic atmosphere and K^+ ions facilitating stable SO_2 adsorption on carbon. Due to potassium, the chemicals created on the surface during adsorption include stable ionic crystals such as K_2SO_3 and K_2SO_4. This is because potassium is highly reactive and cannot exist as a single element; instead, potassium exists in chemical compounds [28]. Previous studies on the properties of carbon surfaces after SO_2 adsorption indicate that strong chemical interactions between KOH and SO_2 largely depend on the impregnated carbon's surface chemistry.

3.5. Stability of the Spent Activated Carbon

Based on the information for the surface functional groups obtained from the FTIR analysis, the presence of adsorbed substances on the used AC-P was also examined using XRD analysis. The XRD analysis allowed us to identify the substances formed on the surface of the activated carbon after SO_2 adsorption. Figure 7 shows the XRD spectra for fresh and used AC-P. For fresh AC-P, a high-intensity peak (2θ = 26.5) was observed. This peak was not seen on any of the used AC-Ps. This peak may indicate the presence of potassium and basic OH ions (AC impregnated with KOH) on the external surface of fresh AC-P that disappeared after SO_2 adsorption. The XRD spectra of all the used AC-Ps indicated the presence of K_2SO_4 generated as a result of a reaction between sulfur oxides and potassium hydroxide (high-intensity peak at 2θ = 30.7), whereas high-intensity peaks at 2θ = 21.24, 29.7, 30.74, and 43.36 as well as small intensity peaks at 35.8 and 37.04 were observed in all the samples after SO_2 adsorption.

Figure 7. The XRD spectra of activated carbon (fresh and after use in the $deSO_x$ and $deNO_x$ adsorber): fresh AC-P, used AC-P (1), used AC-P (2) and used AC-P (3).

Figure 8a,b shows the TG and DTG curves of activated carbon (fresh AC-P and AC-P after use in the $deSO_x$ and $deNO_x$ adsorber) under an inert atmosphere (N_2). As shown in Figure 8a, each sample was characterized by varying the mass loss during the experiment. The greatest mass loss was observed for activated carbon with AC-P (1) after use in the $deSO_x$ and $deNO_x$ adsorber. The loss amounted to 35%, whereas fresh AC-P's mass loss was 20%. As indicated by the TG/DTG curves (Figure 8a,b), two types of mass loss were observed in the fresh AC-P sample. The first type of mass loss was due to the desorption of physically adsorbed water. The second type of mass loss (200–1000 °C) resulted from the slow thermal decomposition of the surface functional groups with low stability and the least thermally stable carbon structure.
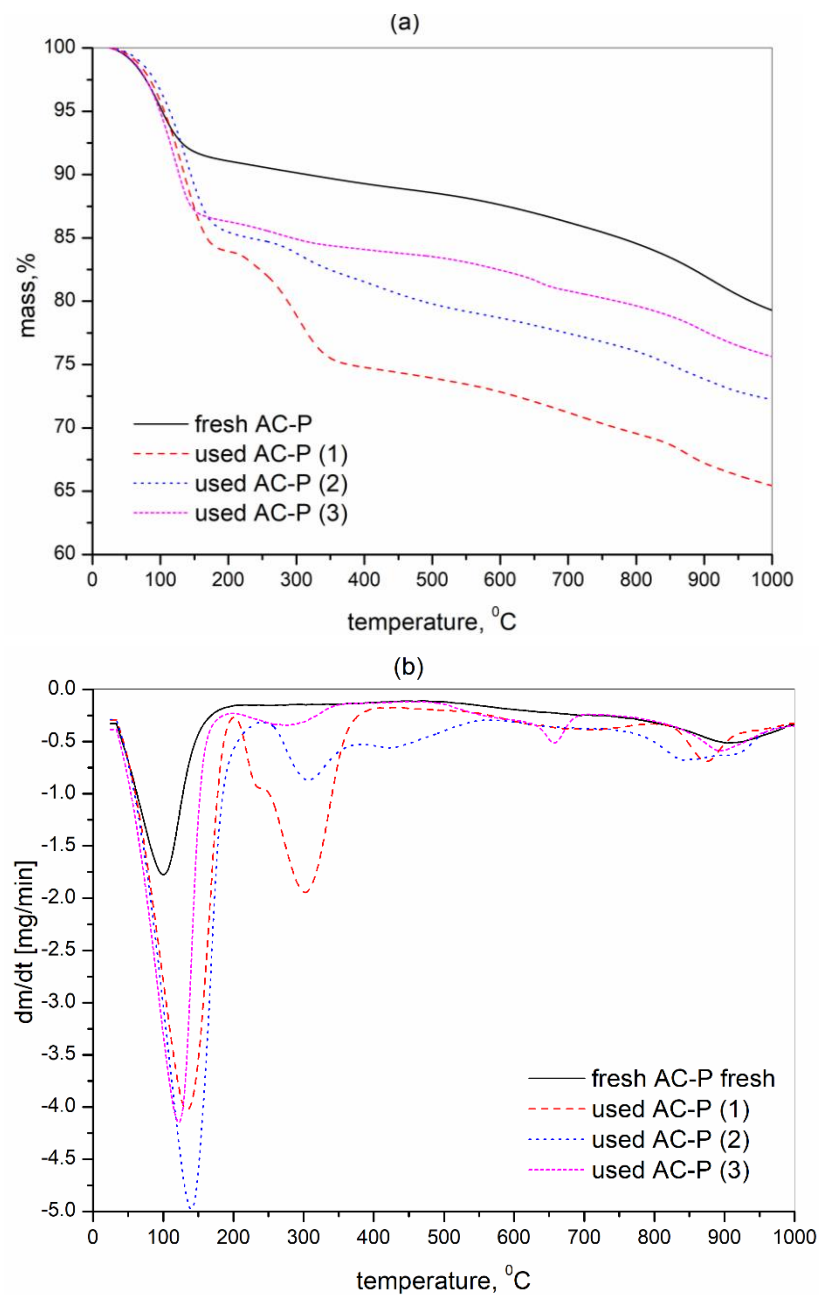
Figure 8. TG (**a**) and DTG (**b**) curves of activated carbon (fresh and after use in the $deSO_x$ and $deNO_x$ adsorber): fresh AC-P, used AC-P (1), used AC-P (2), and used AC-P (3).

Different situations were observed for all spent AC-P-activated carbon. As indicated by the TG/DTG curves (Figure 8a,b), four types of mass loss were observed in the spent AC-

P samples. The first type of mass loss (30–200 °C) was due to the desorption of surface water. The second type of mass loss (200–400 °C) resulted from the removal of water from the pores of the adsorbent. The third type of mass loss (440–650 °C) was due to the desorption of sulfur. The fourth type of mass loss (>650 °C) resulted from the decomposition of potassium sulfate. All completed analyses demonstrated that the mechanism of deep flue gas purification on the activated carbon using AC-P involved the reaction of SO_2 to K_2SO_3 and, through oxidation of SO_2 to SO_3 and adsorption, a reaction to K_2SO_4. The presence of these compounds was confirmed by XRD, SEM-EDX, and TG analyses. However, the presence of nitrogen oxide removal products was not observed, indicating that nitrogen oxides, especially NO, were not oxidized in the desulfurization unit to N_2O_5 and N_2O_4 and thus did not react with KOH to produce potassium nitrites and nitrates (KNO_2, KNO_3). The FTIR, XRD, SEM-EDX, and TG analyses also did not confirm the existence of these compounds. A previous study carried out by the present authors also confirmed that NO_x was not removed from flue gas before CO_2 adsorption in a special section [9]. According to these studies, a large part of the NO_x was adsorbed—not in the desulfurization and NO_x removal section, but in the CO_2 separation section, thus contaminating the activated carbon. The used activated carbon materials (in the four adsorption columns—CO_2 separation section) featured increased nitrogen content, which suggested the slight adsorption of NO_x captured from the flue gas. Details of this analysis can be found in [9]. Many of the same results were obtained by Lee et al. [29] during a study on the surface of impregnated activated carbon after NO_x and SO_2 adsorption. The authors observed that in most cases, adsorption proceeded during chemical reactions. Due to the presence of OH groups on the surface, the KOH-impregnated activated carbon oxidized due to NO_x and SO_2 adsorption. In particular, SO_2 presented strong interactions with KOH-impregnated activated carbon, forming K_2SO_4 on the external surface of activated carbon. Lee et al. [29] also observed that more SO_2 adsorbed on the surface of KOH-impregnated activated carbon corresponded to less NO_x being adsorbed. The authors in [29] showed that the individual adsorption of NO_x and SO_2 proceeded differently than the simultaneous adsorption of both impurities. Many of the same conclusions were presented by Abdulrasheed et al. [27], who observed that the simultaneous removal of NO_x and SO_2 using KOH-impregnated activated carbon in an environment rich in O_2 showed SO_2 to have higher affinity to the adsorbent than NO_x. This was likely also the case in our research. On the other hand, when these gases were removed separately, NO_x showed higher affinity than SO_2. The stronger affinity of SO_2 ensured a higher rate of chemisorption on the surface of impregnated activated carbon and the bonding of oxygen groups (needed for NO oxidation and further NO_2 adsorption on activated carbon), especially in the presence of moisture and sulfuric acid formation. The conducted research shows that the practical use of technology involving the simultaneous removal of both SO_2 and NO_x still makes flue gas desulfurization and denitrification challenging and requires significant research in this area. This result was also confirmed by the study of Neathery et al. [30] on selective NO_x capture from flue gas containing SO_2, CO_2, H_2O, O_2, and N_2. Neathery et al. observed that NO_x can be selectively adsorbed from flue gas mixtures, but only under the proper conditions—i.e., a sufficiently high oxygen concentration, low SO_2 concentration, and a proper temperature range of 35–120 °C. This suggests that under our real research conditions on simultaneous SO_2 and NO_x adsorption from flue gas, the above conditions were not met, leading NO_x adsorption to be minimal. The conclusions of the study highlight that the simultaneous removal of both SO_2 and NO_x from real CFB flue gas on impregnated activated carbon is still challenging and dependent on the particular conditions of the flue gas.

3.6. Analysis of Flue Gas Constitution before and after Leaving the Adsorber

Information obtained based on analysis of the physicochemical properties of AC-P before and after use in the $deSO_x$ and $deNO_x$ adsorber was also confirmed by analyzing the flue gas constitution before and after leaving the adsorber (marked as points 1 and 2 in Figure 2). Figure 9a shows that before entering the adsorber, almost all the SO_2 contained

in the flue gas was captured via impregnated AC-P, and the volume of SO_2 in flue gas leaving the adsorber did not exceed 5 mg/Nm^3 (SO_2 content at the adsorber inlet was 1–111 mg/Nm^3).
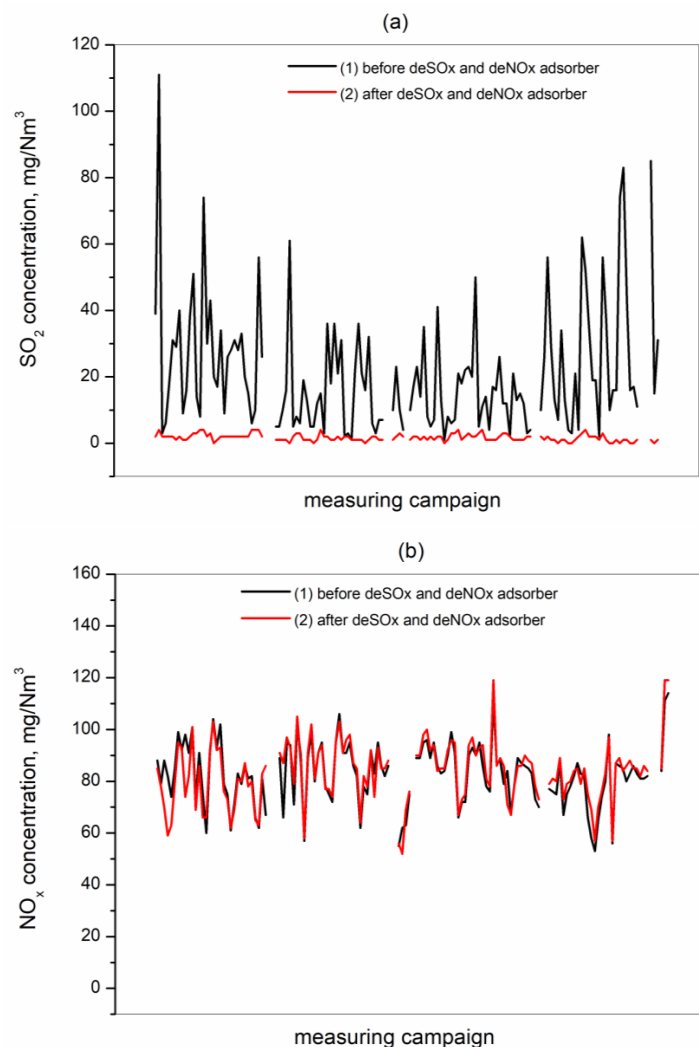
Figure 9. Online analysis of SO_2 concentration (**a**) and NO_x concentration (**b**) in the flue gas before and after leaving the deSO$_x$ and deNO$_x$ adsorber (the temperature of the CFB flue gas was 25 °C, the maximum capacity of the DR-VPSA installation was 100 Nm^3/h, the measuring campaign was 808 h).

This result confirmed the efficacy of desulfurization in the deSOx and deNOx adsorber. The total SOx removal efficiency amounted to 95.5–100%. Similar results were reported by Ishibashi et al. [4,5]. In [4,5], SO_2 removal was so effective that no SO_2 accumulation was observed in the CO_2 adsorbent removed after 2000 h of use in a PTSA/PSA adsorption installation for CO_2 capture. The authors also stated that for CO_2 capture VPSA processes, installing a SOx desulfurization and NOx removal section was less expensive than accepting the adsorbent degradation when the flue gas contained more than 10 mg/Nm3 SO_2 and 10 mg/Nm3 NOx [4,5]. Our analysis of the adsorbent also confirmed the effective removal of SO_2 in the pre-treatment section. Replacement of the AC-P sorbent that filled the deSOx/deNOx adsorber was not necessary after 808 h of DR-VPSA operation because no increase in the SO_2 concentration at the outlet of the column was observed. This result confirmed the effectiveness and lifespan of the adsorbent used to remove SO_2. However, the situation was different for nitrogen oxides, which were not captured in the adsorber, as shown in Figure 9b. The content of nitrogen oxides in the flue gas (reaching

55–120 mg/Nm^3 before entering the adsorber) dropped by only a few mg/Nm^3 after leaving the adsorber. However, it never exceeded 120 mg/Nm^3. In a previous study completed by the same authors of the present work [9], uncaptured NO$_x$ progressed to the CO$_2$ separation section (DR-VPSA), where it was adsorbed on the CO$_2$ adsorbent and as a result of cyclic sorption/desorption processes, mixed with recirculating gas and ultimately appeared as impurities in the final CO$_2$ product [8]. This result confirmed that the process of removing NOx in desulfurization and the NOx removal section was ineffective.

4. Conclusions

The present results based on real CFB flue gas at the Lagisza Power Plant demonstrated that using AC impregnated with KOH and KJ in the adsorber to remove sulfur and nitrogen oxides in the pre-treatment module of the adsorption CO$_2$ capture unit (DR-VPSA) was a solution that ensured sufficient flue gas purification and the removal of sulfur oxides. However, this method is insufficient for nitrogen oxides. The impregnated activated carbon showed adequate sorptive properties and proper thermal stability. It also did not change its properties during prolonged use in the adsorber. The tested activated carbon allowed for the effective removal of sulfur oxides under the continuous operation of the DR-VPSA installation for variable SO$_2$ and NO$_x$ loading in real flue gas conditions. This was confirmed by completed analyses of the spent activated carbon, which allowed finding the presence of SO$_2$ adsorption products with chemical reaction, as potassium sulfate, on the surface of the spent activated carbon. From among the various alternatives, the removal of impurities from the flue gas through adsorption on surface-modified KOH/KJ activated carbon proved to be an efficient and reliable technology for sulfur oxides. However, the removal of nitrogen oxides under real conditions was not assessed.

References

1. Bhown, A.B.; Freeman, B.C. Analysis and Status of Post-Combustion Carbon Dioxide, Capture Technologies. *Environ. Sci. Technol.* **2011**, *45*, 8624–8632. [CrossRef]
2. International Energy Agency. Carbon Capture, Utilization and Storage, a Critical Tool in the Climate Energy Toolbox. Available online: https://www.iea.org/topics/carbon-capture-and-storage/ (accessed on 25 February 2021).
3. Webley, P.A. Adsorption technology for CO$_2$ separation and capture: A perspective. *Adsorption* **2014**, *20*, 225–231. [CrossRef]
4. Ishibashi, M.; Ota, H.; Akutsu, N.; Umeda, S.; Tajika, M.; Izumi, J.; Yasutake, A.; Kabata, T.; Kageyama, Y. Technology for removing carbon dioxide from power plant flue gas by the physical adsorption method. *Energy Convers. Manag.* **1996**, *37*, 929–933. [CrossRef]
5. Ishibashi, M.; Otake, K.; Kanamori, S.; Yasutake, A. Study on CO$_2$ removal technology from flue gas of thermal power plant by physical adsorption method. In *Greenhouse Gas Control Technologies, Proceedings of the 4th International Conference, Interlaken, Switzerland, 30 August–2 September 1998*; Eliasson, B., Riemer, P., Wokaun, A., Eds.; Elsevier Science Ltd.: Oxford, UK, 1998; pp. 131–136.

6. Wang, L.; Yang, Y.; Shen, W.; Kong, X.; Li, P.; Yu, J.; Rodrigues, A.E. CO₂ capture from flue gas in an existing coal-fired power plant by two successive pilot-scale VPSA units. *Ind. Eng. Chem. Res.* **2013**, *52*, 7947–7955. [CrossRef]

7. Qader, A.; Hoopera, B.; Innocenzib, T.; Stevensc, G.; Kentishc, S.; Scholesc, C.; Mumfordc, K.; Smithc, K.; Webley, P.A.; Zhangd, J. Novel post-combustion capture technologies on a lignite fired power plant-results of the CO2CRC/H3 capture project. *Energy Procedia* **2011**, *4*, 1668–1675. [CrossRef]

8. Wawrzyńczak, D.; Majchrzak-Kucęba, I.; Srokosz, K.; Kozak, M.; Nowak, W.; Zdeb, J.; Smółka, W.; Zajchowski, A. The pilot dual-reflux vacuum pressure swing adsorption unit for CO₂ capture from flue gas. *Sep. Purif. Technol.* **2019**, *209*, 560–570. [CrossRef]

9. Majchrzak-Kucęba, I.; Wawrzyńczak, D.; Ściubidło, A.; Zdeb, J.; Smółka, W.; Zajchowski, A. Stability and regenerability of acivated carbon used for CO₂ removal in pilot DR-VPSA unit in real power plant conditions. *J. CO₂ Util.* **2019**, *29*, 1–11. [CrossRef]

10. Chapel, D.G.; Ernest, J.; Mariz, C.L. Recovery of CO₂ from Flue Gases: Commercial Trends. In Proceedings of the Canadian Society of Chemical Engineers annual meeting, Saskatoon, SK, Canada, 4–6 October 1999.

11. Hu, J.; Liu, Y.; Liu, J.; Gu, C. Effects of water vapor and trace gas impurities in flue gas on CO₂ capture in zeolitic imidazolate frameworks: The significant role of functional groups. *Fuel* **2017**, *200*, 244–251. [CrossRef]

12. Schallert, B.; Satterley, C.; Neuhaus, S. The impact of NO₂ on post-combustion capture: What concentration of NO₂ is expected in front of the absorber and what is its fate in the capture proces? In Proceedings of the 2nd Post Combustion Capture Conference (PCCC2), Bergen, Norway, 7–20 September 2013.

13. Zhang, J.; Xiao, P.; Li, G.; Webley, P.A. Effect of Flue gas impurities on CO₂ capture performance from flue gas at coal-fired power stations by Vacuum Swing adsorption. *Energy Procedia* **2009**, *1*, 115–1122. [CrossRef]

14. Sayari, A.; Belmabkhout, Y.; Serna-Guerrero, R. Flue gas treatment via CO₂ adsorption. *Chem. Eng. J.* **2011**, *171*, 760–774. [CrossRef]

15. Sass, B.; Ricci, S.; Gupta, A.; Hindin, B.; Gupta, N. Impact od SOx and NOx in flue gas on CO₂ separation, compression and pipeline transmission. In *Carbon Dioxide Capture and Storage in Deep Geologic Formations—Results from the CO₂ Capture Project*; Thomas, D.C., Ed.; Elsevier: Amsterdam, The Netherlands, 2005; pp. 955–981.

16. Porter, R.T.J.; Fairwether, M.; Pourkashanian, M. The range and level of impurities in CO₂ streams from different carbon capture sources. *Int. J. Greenh. Gas Control.* **2015**, *36*, 161–174. [CrossRef]

17. Cao, A.; Zhao, H.; Hu, D.; Wang, J.; Li, M.; Zhou, Z.; Shen, Q.; Sun, N.; Wei, W. Preparation of potassium intercalated carbons by in-situ activation and speciation for CO₂ capture from flue gas. *J. CO₂ Util.* **2020**, *35*, 59–66. [CrossRef]

18. Labus, K.; Grygiewicz, K.; Machnikowski, J. Granular KOH-activated carbons from coal-based cokes and their CO₂ adsorption capacity. *Fuel* **2014**, *118*, 9–15. [CrossRef]

19. Li, D.; Zhou, J.; Wang, Y.; Tian, Y.; Wei, L.; Zhang, Z.; Qiao, Y.; Li, J. Effects of activation temperature on densities and volumetric CO₂ adsorption performance of alkali-activated carbons. *Fuel* **2019**, *238*, 232–239. [CrossRef]

20. Sabouni, R.; Kazemian, H.; Rohani, S. Carbon dioxide capturing technologies: A review focusing on metal organic framework materials (MOFs). *Environ. Sci. Pollut. Res.* **2014**, *21*, 5427–5449. [CrossRef] [PubMed]

21. Gargiulo, V.; Alfe, M.; Raganati, F.; Lisi, L.; Chirone, R.; Ammendola, P. BTC-based metal-organic frameworks: Correlation between relevant structural features and CO₂ adsorption performances. *Fuel* **2018**, *222*, 319–326. [CrossRef]

22. Zelenak, V.; Halamowa, D.; Gaberowa, L.; Bloch, E.; Lewellyn, P. Amine-modified SBA-12 mesoporous silica for carbon dioxide capture: Effect of amine basicity on sorption properties. *Micropor. Mesopor. Mater* **2008**, *116*, 358–364. [CrossRef]

23. Wappel, D.; Khan, A.; Shallcross, D.; Joswig, S.; Kentish, S.; Stevens, G. The effect of SO₂ on CO₂ absorption in an aqueous potassium carbonate solvent. *Energy Procedia* **2009**, *1*, 125–131. [CrossRef]

24. Directive 2010/75/EU of the European Parliament and the Council on Industrial Emissions (the Industrial Emissions Directive or IED). Available online: http://data.europa.eu/eli/dir/2010/75/oj (accessed on 20 February 2021).

25. Guo, Y.; Li, Y.; Zhu, T.; Ye, M. Investigation of SO₂ and NO adsorption species on activated carbon and the mechanism of NO promotion effect on SO₂. *Fuel* **2015**, *143*, 536–542. [CrossRef]

26. Qiang, T.; Zhigang, Z.; Wenpei, Z.; Zidong, C. SO₂ and NO selective adsorption properties of coal-based activated carbons. *Fuel* **2005**, *84*, 461–465. [CrossRef]

27. Abdulrasheed, A.A.; Jalil, A.A.; Triwahyono, S.; Zaini, M.A.A.; Gambo, Y.; Ibrahim, M. Surface modification of activated carbon for adsorption of SO₂ and NOx: A review of existing and emerging technologies. *Renew. Sustain. Energy Rev.* **2018**, *94*, 1067–1085. [CrossRef]

28. Lee, Y.W.; Park, J.W.; Choung, J.H.; Choi, D.K. Adsorption Characteristics of SO₂ on Activated Carbon Prepared from Coconut Shell with Potassium Hydroxide Activation. *Environ. Sci. Technol.* **2002**, *36*, 1086–1092. [CrossRef]

29. Lee, Y.W.; Kim, H.J.; Park, J.W.; Choi, B.U.; Choi, D.K. Adsorption and reaction behaviour for the simultaneous adsorption of NO–NO₂ and SO₂ on activated carbon impregnated with KOH. *Carbon* **2003**, *41*, 1881–1888. [CrossRef]

30. Neathery, J.K.; Rubel, A.M.; Stencel, J.M. Uptake of NOx by activated carbons: Bench-scale and pilot-plant testing. *Carbon* **1997**, *35*, 1321–1327. [CrossRef]